

Experimental and Theoretical Study of Novel Luminescent Di-, Tri-, and Tetranuclear Copper Triazole Complexes

Daniel M. Zink,[†] Tobias Grab,[‡] Thomas Baumann,^{*,‡} Martin Nieger,[§] Ericka C. Barnes,^{||} Wim Klopper,[⊥] and Stefan Bräse^{*,†}

[†]Institute of Organic Chemistry, Karlsruhe Institute of Technology, KIT Campus South, Fritz-Haber-Weg 6, D-76131 Karlsruhe, Germany

[‡]cynora GmbH, Hermann-von-Helmholtz-Platz 1, D-76344 Eggenstein-Leopoldshafen, Germany

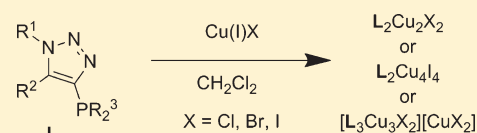
[§]Laboratory of Inorganic Chemistry, Department of Chemistry, University of Helsinki, P.O. Box 55 (A.I. Virtasen aukio 1), FIN-00014 University of Helsinki, Finland

^{||}Institute of Nanotechnology, Karlsruhe Institute of Technology, KIT Campus North, Hermann-von-Helmholtz-Platz 1, D-76344 Eggenstein-Leopoldshafen, Germany

[⊥]Institute of Physical Chemistry, Karlsruhe Institute of Technology, KIT Campus South, Fritz-Haber-Weg 2, D-76131 Karlsruhe, Germany

S Supporting Information

ABSTRACT: A number of novel luminescent di-, tri-, and tetranuclear copper complexes have been synthesized in good yields using a modular ligand system based on triazole-phosphines. This kind of ligand is easily accessible through an improved one-pot synthesis that permits the facile introduction of various alkyl or aromatic substituents at the 1-, 4-, or 5-position of the triazole ring. X-ray crystallography revealed three different types of complexes: neutral di- and tetranuclear structures with C_i symmetry, and a charged trinuclear structure possessing C_3 symmetry. A spectroscopic evaluation showed promising photoluminescence properties in terms of their potential use in organic light-emitting devices, with maxima in the range of 500–550 nm, depending on the substitution pattern of the triazole ligand used for the complexation. Experimental observations were complemented by density functional theory calculations of ground and excited states.



INTRODUCTION

Luminescent metal complexes have recently been the focus of many scientific investigations, owing to their potential use as organic light-emitting diodes,¹ solar cells,² and chemical sensors,^{3,4} to name a few. Highlighting their application as organic light-emitting diodes, a great number of these luminescent complexes have been shown to significantly increase the luminosity of the diode, such as in the case of triplet emitters. The second- and third-row transition metals are commonly employed as the central core of the complex, the most noteworthy of these being platinum,⁵ ruthenium,⁶ osmium,⁶ and iridium.⁷ Coupled with certain ligands, triplet emitters employing these transition metals have been shown to possess extraordinarily high efficiencies. A downside to utilizing these metals, however, is their inaccessibility; they are quite rare and expensive. For industrial applications in mass markets, e.g., flat screens or other novel lighting applications, the development of novel complexes that not only possess characteristics similar to those of triplet emitters, but also fulfill economic and environmental considerations, becomes necessary. Therefore, in the past few years, the search for more abundant and economical luminescent complexes has intensified. The main focus of this research is on metals with d^{10} configurations, such as Cu(I), Ag(I), Au(I), Zn(II), and Cd(II),

due to their abundance and ability to form a wide range of luminescent complexes.⁸ Among the examples mentioned above, copper complexes represent the most prolific group of luminescent metal compounds. Thus, complexes with chelating bisimine ligands of the general composition $[\text{Cu}(\text{N}\wedge\text{N})_2]^+$, e.g. substituted bisphenanthroline **1** (Figure 1), are widely reported in the literature. Other promising complexes possess the general composition $[\text{Cu}(\text{P}\wedge\text{P})_2]^+$, $[\text{Cu}(\text{N}\wedge\text{N})(\text{P}\wedge\text{P})]^+$, and/or $[\text{Cu}(\text{N}\wedge\text{N})(\text{P}\wedge\text{N})]^+$, together with chelating phosphine ligand **2** and/or heteroleptic ligand **3**^{8,9} (Figure 1).

Luminescent complexes of triazole ligands with ruthenium,¹⁰ iridium,^{10,11} platinum,¹² osmium,¹³ and copper¹⁴ are also well-known. In contrast to this, however, little is known about luminescent complexes with the ClickPhos ligand **4** (Figure 1), in spite of great potential owing to their simple and economical preparation, good optical characteristics, and modal structure.

Most of the complexes described above are mononuclear, but dinuclear and trinuclear metal complexes, such as those involving platinum¹⁷ or rhenium,¹⁸ have recently gained attention as potential novel optical materials. In this study, we report on

Received: December 10, 2010

Published: May 20, 2011

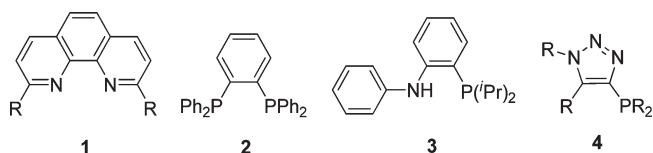


Figure 1. Different N \wedge N, P \wedge P, and N \wedge P ligands.

Scheme 1. Synthesis of ClickPhos-like triazole ligands 2¹⁹

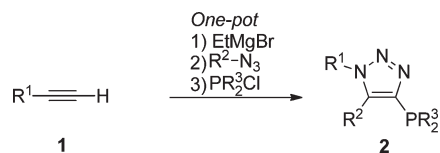


Table 1. ClickPhos-ligands Synthesized To Furnish Various Copper Triazole Complexes

compd	R ¹	R ²	R ³
2a	Ph	Ph	Ph
2b	Bn	Ph	Ph
2c	hexyl	Ph	Ph
2d	2-phenylethyl	Ph	Ph
2e	Ph	propyl	Ph
2f	Bn	propyl	Ph
2g	hexyl	propyl	Ph
2h	Ph	naphthyl	Ph
2i	4-nitrophenyl	Ph	Ph
2j	Ph	3-chlorophenyl	Ph
2k	Ph	Ph	C ₆ F ₅

the synthesis and structure of new polynuclear and luminescent complexes of various ClickPhos-type ligands with copper as the central metal.

SYNTHESIS OF LIGANDS AND COMPLEXES

For the synthesis of the different di-, tri-, and tetranuclear copper triazole complexes, we used a modular ligand system based on ClickPhos-like 1,4,5-trisubstituted triazoles. Most of these ligands are accessible not only according to the Sharpless or Zhang reactions via a two-step procedure,^{15,16} but also, more conveniently, by an easy-to-handle and straightforward one-pot reaction.¹⁶ In our previous work, we not only improved on this method (Scheme 1),¹⁹ but also synthesized all of the 1,4,5-trisubstituted triazoles **2a–k** summarized in Table 1 in moderate to good yields.

The selection of ligands was based on two central considerations: those of electronic effects and substitution pattern. First, a set of triazole ligands with various electronic characteristics was synthesized in order to determine electronic influences. This set consisted of azides, alkynes, and phosphines with different electron-withdrawing and -donating substituents. The substituents at two positions of the triazole were retained, while the third substituent was varied in order to examine the electronic effects of electron-poor and electron-rich triazole ligands on their corresponding luminescence spectra. Second, trends in the luminescence spectra were examined by varying the substituents

Scheme 2. Synthesis of the Copper Triazole Complexes 3a–o

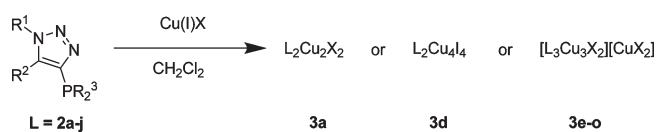


Table 2. Synthesized Copper Triazole Complexes

ligand	metal salt	complex	stoichiometry ^a	color
2a	CuI	3a	L ₂ Cu ₂ I ₂	colorless
2a	CuBr	3b	[L ₃ Cu ₃ Br ₂][CuBr ₂]	colorless
2a	CuCl	3c	[L ₃ Cu ₃ Cl ₂][CuCl ₂]	colorless
2a	CuI	3d	L ₂ Cu ₄ I ₄	colorless
2a	CuI	3e	[L ₃ Cu ₃ I ₂][CuI ₂]	colorless
2b	CuI	3f	[L ₃ Cu ₃ I ₂][CuI ₂]	colorless
2b	CuBr	3g	[L ₃ Cu ₃ Br ₂][CuBr ₂]	gray
2b	CuCl	3h	[L ₃ Cu ₃ Cl ₂][CuCl ₂]	gray
2c	CuI	3i	[L ₃ Cu ₃ I ₂][CuI ₂]	colorless
2d	CuI	3j	[L ₃ Cu ₃ I ₂][CuI ₂]	colorless
2e	CuI	3k	[L ₃ Cu ₃ I ₂][CuI ₂]	colorless
2g	CuI	3l	[L ₃ Cu ₃ I ₂][CuI ₂]	colorless
2h	CuI	3m	[L ₃ Cu ₃ I ₂][CuI ₂]	colorless
2i	CuI	3n	[L ₃ Cu ₃ I ₂][CuI ₂]	orange
2j	CuI	3o	[L ₃ Cu ₃ I ₂][CuI ₂]	colorless

^aBased on mass spectroscopy and X-ray crystallography (for **3a,d,k**).

at the 1- or 5-position. This was achieved by replacing an alkyl substituent with a phenyl ring. In doing so, one can reveal the extent at which the steric characteristics of the ligands affect the complexation.

The synthesis of the complexes was carried out by reaction of the triazole ligands with the corresponding amount of copper halide in dichloromethane, with the complexation being completed after a few hours. The purification of the complexes was accomplished by precipitation of the filtered reaction mixture in cyclohexane. The complexes given in Table 2 were obtained in high purity and moderate yields.

For the 4-(diphenylphosphino)-1,5-diphenyl-1*H*-1,2,3-triazole (**2a**) and 1-benzyl-4-(diphenylphosphino)-5-phenyl-1*H*-1,2,3-triazole (**2b**) ligands, copper(I) iodide as well as copper(I) bromide and chloride, were used as metal salts. Members of the homologous series of triazole copper halide complexes were investigated, in order to gain further understanding of the trends in structural and electronic effects. Only copper(I) iodide was used as the metal salt in the preparation of all other trisubstituted triazole copper complexes (Table 2), however, as the luminescence of these complexes proved to be more intense than those of the corresponding copper(I) bromide and chloride complexes. The reaction of 4-(bis(perfluorophenyl)phosphino)-1,5-diphenyl-1*H*-1,2,3-triazole (**2k**) with copper(I) iodide showed no complexation, most likely due to the electron-withdrawing effect of the electronegative fluorine atoms that also serve to lower the electron density of the phosphorus atom. Furthermore, the reactions of different triazoles with copper(I) cyanide did not result in the formation of a copper complex, further demonstrating the ability of halogen atoms to act as bridging ligands.

STRUCTURE OF COMPLEXES

The three-dimensional structures of the three di-, tri-, and tetranuclear copper triazole complexes were determined by X-ray structure analysis. Complex **3a**, with 4-(diphenylphosphino)-1,5-diphenyl-1*H*-1,2,3-triazole (**2a**) as the ligand and copper(I) iodide as the metal salt, was obtained by recrystallization from ethyl acetate. The X-ray structure analysis points to a dinuclear, C_i -symmetric complex composed of two ligand molecules and two molecules of copper(I) iodide. The copper(I) and the μ_2 -iodide ions form a distorted square plane, in which the copper(I) and the iodide ions each occupy opposite corners. The two ligands coordinate only the copper(I) ions via their respective phosphorus atoms and do not make use of any of the triazole nitrogen atoms for further coordination to the metal core, as might otherwise be expected. In addition, the copper–copper distance of 2.60 Å suggests that a direct metal–metal interaction exists between the two copper(I) ions, serving to coordinatively saturate the metal. The influence of the bridging iodine ions on the copper–copper distance and possible binding interactions in this kind of Cu_2I_2 core has been extensively examined by Caulton et al.²⁰ and, based on this work, a metal–metal interaction in complex **3a** is possible. The two phenyl substituents at the C-5 atom of the triazole are nearly parallel to the planar copper(I) iodide square, forming a

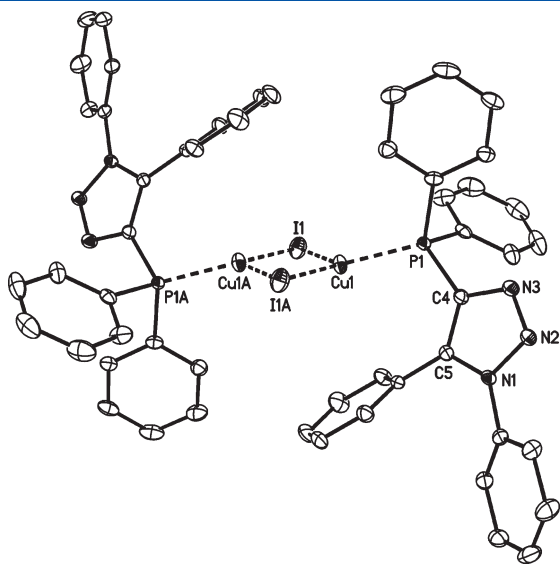


Figure 2. Molecular structure of [(4-(diphenylphosphino)-1,5-diphenyl-1*H*-1,2,3-triazole)₂Cu₂I₂] (**3a**) (hydrogen atoms omitted for clarity, displacement parameters drawn at the 50% probability level).

sandwich-like structure. Figure 2 shows the crystal structure of this complex. Selected bond lengths and angles are summarized in Table 3.

The measured copper–copper bond length of 2.60 Å is within the range of the copper–copper distance in the bulk metal (2.56 Å) and those of other copper complexes with direct metal–metal interactions (2.55–2.72 Å),²¹ and is even shorter than in complexes with the same kind of Cu_2I_2 core and assumed copper interactions.^{20,22} The assumption of a direct metal–metal interaction is further supported by the fact that the copper atom is coordinated to only three ligands and is therefore capable of forming a metal–metal bond.

The tetranuclear copper complex **3d** was obtained under slightly different conditions (i.e. diffusion of diethyl ether in dichloromethane solution). Its structure was determined by X-ray crystallography. In contrast to the previous complex, a P–N motif was formed (Figure 3). In this tetranuclear, C_i -symmetric complex consisting of two molecules of 4-(diphenylphosphino)-1,5-diphenyl-1*H*-1,2,3-triazole and four copper and four iodine ions, the four coppers and two of the iodides form an octahedron, with the four copper(I) atoms spanning the base and the two iodides occupying the remaining axial positions. Each of the two remaining iodides acts as a bridging ligand between two copper(I) atoms. The two 4-(diphenylphosphino)-1,5-diphenyl-1*H*-1,2,3-triazole ligands coordinate through their phosphorus atom and the nitrogen atom at the 3-position of the triazole ring as chelating ligands between two copper(I) atoms. Due to steric reasons, the two ligands and the two iodides occupy positions opposite from each other. Each

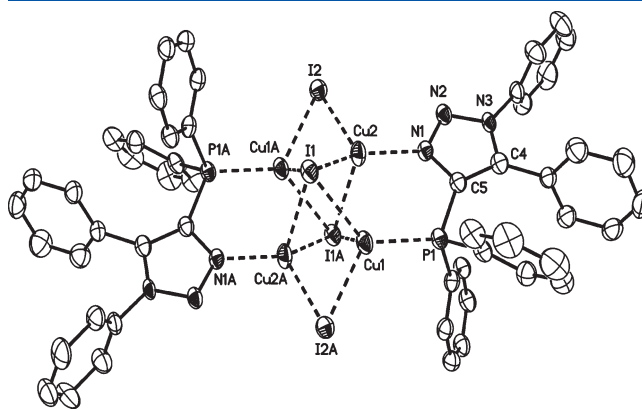


Figure 3. Molecular structure of [(4-(diphenylphosphino)-1,5-diphenyl-1*H*-1,2,3-triazole)₂Cu₄I₄] (**3d**) (hydrogen atoms omitted for clarity, displacement parameters drawn at the 50% probability level).

Table 3. Selected Bond Lengths and Angles of Complex **3a**^a

Bond Lengths (Å)			
I(1)–Cu(1)	2.5466(7) [2.636]		2.5965(6) [2.625]
I(1)–Cu(1A)#1	2.5965(6) [2.625]	Cu(1)–Cu(1A)#1	2.6001(8) [2.586]
Cu(1)–P(1)	2.2118(9) [2.268]		
Bond Angles (deg)			
Cu(1)–I(1)–Cu(1A)#1	60.73(2) [58.9]	P(1)–Cu(1)–I(1A)#1	115.86(3) [118.6]
P(1)–Cu(1)–I(1)	122.43(3) [119.3]	I(1)–Cu(1)–I(1A)#1	119.27(2) [121.1]

^a The corresponding values computed at the BP86/def2-SV(P) level are given in brackets. Symmetry transformations used to generate equivalent atoms: (#1) $-x + 1, -y + 1, -z + 1$.

Table 4. Selected Bond Lengths and Angles of Complex 3d^a

Bond Lengths (Å)			
I(1)–Cu(1)	2.5885(9)	Cu(1)–Cu(2A)#1	2.5398(10)
I(1)–Cu(2)	2.6358(9)		2.5881(9)
I(1)–Cu(2A)#1	2.9679(10)	Cu(1)–Cu(2)	2.8818(11)
I(1)–Cu(1A)#1	3.2472(9)		3.2472(9)
I(2)–Cu(1A)#1	2.5881(9)	Cu(2)–N(1)	1.983(4)
I(2)–Cu(2)	2.6005(9)		2.5398(10)
Cu(1)–P(1)	2.2001(16)		2.9679(10)
Bond Angles (deg)			
Cu(1)–I(1)–Cu(2)	66.95(3)	I(2A)#1–Cu(1)–I(1)	111.29(3)
Cu(1)–I(1)–Cu(2A)#1	53.88(2)	P(1)–Cu(1)–I(1)#1	96.14(4)
Cu(2)–I(1)–Cu(2A)#1	80.84(3)	I(2A)#1–Cu(1)–I(1A)#1	93.05(3)
Cu(1)–I(1)–Cu(1A)#1	86.59(3)	I(1)–Cu(1)–I(1A)#1	93.41(3)
Cu(2)–I(1)–Cu(1A)#1	49.83(2)	N(1)–Cu(2)–I(2)	114.59(13)
Cu(2A)#1–I(1)–Cu(1A)#1	55.03(2)	N(1)–Cu(2)–I(1)	124.21(13)
Cu(1A)#1–I(2)–Cu(2)	58.61(3)	I(2)–Cu(2)–I(1)	108.84(3)
P(1)–Cu(1)–Cu(2A)#1	147.11(5)	N(1)–Cu(2)–I(1A)#1	105.75(13)
P(1)–Cu(1)–I(2A)#1	119.45(5)	I(2)–Cu(2)–I(1A)#1	100.05(3)
P(1)–Cu(1)–I(1)	127.58(5)	I(1)–Cu(2)–I(1A)#1	99.16(3)

^aSymmetry transformations used to generate equivalent atoms: (#1) $-x + 3/2, -y + 1/2, -z + 1$.

copper(I) atom is tetrahedrally coordinated by three iodides and either a nitrogen or a phosphorus atom. The rectangular base of the octahedron composed of the four copper ions has two side lengths measuring 2.53 and 2.88 Å (Table 4). The two shorter bonds at 2.53 Å feature the iodides as μ_2 ligands, while the triazole ligands act as μ_2 ligands in the case of the two longer bonds. As mentioned above, such a bridging coordination of an iodide might be an indication of a metal–metal interaction. This assumption is supported by the relatively short copper–copper distances. Of the Cu–Cu bond distances of 2.53 and 2.88 Å, the latter may still be characterized as a direct interaction, based on comparisons with the Cu–Cu bond length in bulk metal and other similar complexes.

However, in this kind of complex, the copper(I) atoms are coordinatively saturated, and a direct metal–metal interaction is therefore not very likely. Even though the bond lengths I(1)–Cu(1A) and I(1A)–Cu(1) at 3.25 Å might seem too long for strong interactions to be present, it is quite reasonable to assume that weak interactions do exist to coordinatively saturate the copper ions. This type of Cu_4I_4 core has been described in the literature. Mezailles et al.²³ and Fu et al.²⁴ synthesized analogous complexes with either 2-diphenylphosphino-3-methylphosphine or bis-(dicyclohexylphosphino)methane as the bridging ligand, with the resulting copper–iodide bond distances for the μ_4 -iodide within the range of 2.68–2.88 Å. In contrast, a similar complex reported by Camus et al.²⁵ with bis(diphenylphosphino)methane shows only a μ_3 -iodide, with the distance between this iodide and the noncoordinated copper ion being about 3.34 Å. Therefore, under the assumption of a μ_4 -coordinating iodide in the case of complex 3d, the fourth coordination mode could only be a very weak interaction.

Single crystals of a complex from the reaction of 4-(diphenylphosphino)-1-phenyl-5-propyl-1*H*-1,2,3-triazole (2e) with copper(I) iodide were obtained by slow diffusion of diethyl ether in a saturated dichloromethane solution. The X-ray structure analysis confirmed the presence of a charged, trinuclear metal

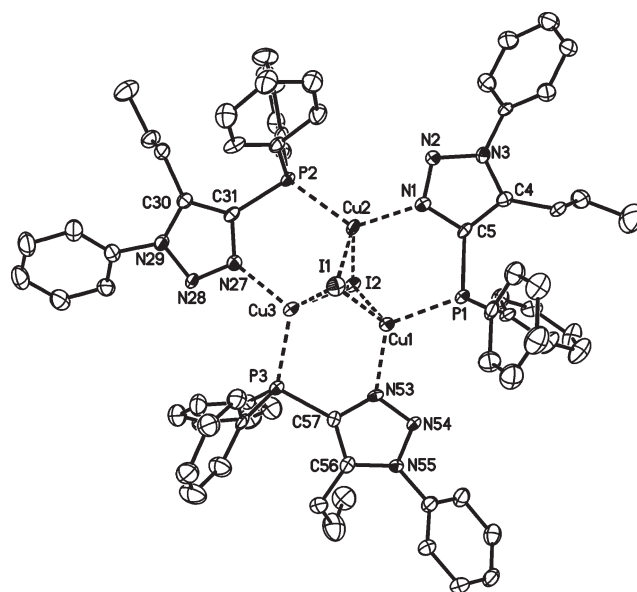


Figure 4. Structure of the cationic of complex 3k (anion, solvent, minor disordered part and hydrogen atoms omitted for clarity, displacement parameters drawn at the 50% probability level).

complex, [(4-(diphenylphosphino)-1-phenyl-5-propyl-1*H*-1,2,3-triazole)₃Cu₃I₂][CuI₂] (3k), consisting of three ligands, namely: 2e, four copper(I) ions, and four iodides. In the positively charged ion [(4-(diphenylphosphino)-1-phenyl-5-propyl-1*H*-1,2,3-triazole)₃Cu₃I₂]⁺, having C₃ symmetry, three copper(I) ions and two iodides form a trigonal bipyramid, in which the three copper(I) ions form the plane, with the two iodides occupying the remaining positions (Figure 4). Even though the single crystals obtained were average in quality, the structure of the complex was nevertheless unequivocally

Table 5. Selected Bond Lengths and Angles of Complex 3k^a

Bond Lengths (Å)			
I(1)–Cu(1)	2.7048(16) [2.746]	Cu(1)–Cu(3)	2.6633(19) [2.636]
I(1)–Cu(3)	2.7114(15) [2.746]	Cu(1)–Cu(2)	2.8158(18) [2.636]
I(1)–Cu(2)	2.7599(15) [2.746]	Cu(2)–N(1)	2.002(9) [2.041]
I(2)–Cu(2)	2.6870(15) [2.778]	Cu(2)–P(2)	2.210(3) [2.279]
I(2)–Cu(1)	2.6894(16) [2.778]	Cu(2)–Cu(3)	2.8195(18) [2.636]
I(2)–Cu(3)	2.7329(15) [2.778]	Cu(3)–N(27)	2.015(9) [2.041]
Cu(1)–N(53)	2.021(9) [2.041]	Cu(3)–P(3)	2.228(3) [2.279]
Cu(1)–P(1)	2.206(3) [2.279]		
Bond Angles (deg)			
Cu(1)–I(1)–Cu(3)	58.91(4) [57.4]	N(1)–Cu(2)–P(2)	125.4(3) [116.5]
Cu(1)–I(1)–Cu(2)	62.02(4) [57.4]	N(1)–Cu(2)–I(2)	103.6(3) [106.2]
Cu(3)–I(1)–Cu(2)	62.03(4) [57.4]	P(2)–Cu(2)–I(2)	112.06(8) [108.4]
Cu(2)–I(2)–Cu(1)	63.17(4) [56.7]	N(1)–Cu(2)–I(1)	106.8(3) [108.5]
Cu(2)–I(2)–Cu(3)	62.69(4) [56.7]	P(2)–Cu(2)–I(1)	100.55(9) [104.3]
Cu(1)–I(2)–Cu(3)	58.83(4) [56.7]	I(2)–Cu(2)–I(1)	107.32(5) [113.1]
N(53)–Cu(1)–P(1)	120.3(3) [116.5]	N(27)–Cu(3)–P(3)	118.1(3) [116.5]
N(53)–Cu(1)–I(2)	101.7(3) [106.2]	N(27)–Cu(3)–I(1)	105.6(3) [108.5]
P(1)–Cu(1)–I(2)	109.31(9) [108.4]	P(3)–Cu(3)–I(1)	113.43(9) [104.3]
Cu(3)–Cu(1)–I(2)	61.40(4) [61.7]	N(27)–Cu(3)–I(2)	105.8(3) [106.2]
N(53)–Cu(1)–I(1)	115.1(3) [108.5]	P(3)–Cu(3)–I(2)	105.79(9) [108.4]
P(1)–Cu(1)–I(1)	101.37(9) [104.3]	I(1)–Cu(3)–I(2)	107.40(5) [113.1]
I(2)–Cu(1)–I(1)	108.86(5) [113.1]		

^a The corresponding values computed at the BP86/def2-SV(P) level are given in brackets.

determined: each copper(I) is coordinated to the two iodine ions, a nitrogen, and a phosphorus atom, collectively forming a flattened tetrahedral structure. Once again, the short copper–copper distance of 2.66–2.82 Å, which is within the range of the sum of the van der Waals radii (2.80 Å),²⁶ suggests the existence of a metal–metal interaction. The copper–iodine distances in this kind of complex are almost equal, differing by 0.05 Å at most (Table 5). Each ligand acts as a chelating ligand and coordinates to both copper ions via the phosphorus atom and the nitrogen atom at the 3-position of the triazole ring. The dinegative counterion [Cu₂I₄]²⁻ is a planar rectangle consisting of four iodides, with both copper(I) ions lying on one of the diagonals of the rectangle. Consequently, each copper ion is coordinated by three iodides and the other copper ion. Upon examination of the literature, very few complexes with such a Cu₃I₂ core have been studied. To the best of our knowledge, the only two examples have been described by Nardin et al.,²⁷ with two bis-(diphenylphosphino)methanes and one iodine as bridging ligands, and Zhou et al.,²⁶ with three bis(diphenylphosphino)methane ligands. The bond lengths and angles of these complexes are in good agreement with the values for complex 3k.

The analysis of the mass spectrometric data of all copper triazole complexes indicates the exclusive formation of the charged trinuclear complex. All mass spectra of the complexes show very similar fragmentation patterns, in that several or all of the following fragmentation signals occur: L₃Cu₃X₂, L₂Cu₃X₂, LCu₃X₂, L₂Cu₂X, L₂Cu, (L–N₂)Cu. This observation confirms that the form [(triazole)₃Cu₃X₂][CuX₂] is preferred by the copper(I) triazole complexes (X = I, Br, Cl).

Since the complexes 3a,d,k feature an almost identical ligand system, a rational explanation might be based on solvent or steric

effects. All of the complexes have been synthesized and purified as described above with a ligand to copper halide ratio of 3:2. Single crystals were obtained either by recrystallization from ethyl acetate (complex 3a) or through diffusion of diethyl ether in dichloromethane (complexes 3d,k). Given the similar structural motif of complexes 3d,k, which differs significantly from that of complex 3a, a solvent effect is thought to be responsible for the formation of the different kinds of complexes. Complex 3a is subject to harsh conditions during recrystallization in hot ethyl acetate due to its low solubility. These conditions result in a change in structure from a charged trinuclear basic structure such as 3k to the uncharged, dinuclear structure that was revealed by X-ray analysis. This rearrangement was proven by elemental analysis before and X-ray structure analysis after the recrystallization process. Taking this observation into account, a polar solvent such as ethyl acetate seems to promote the formation of a complex such as 3a, while in a less polar solvent combination such as diethyl ether/dichloromethane, the formation of complexes such as 3d,k might be favored. Theoretical calculations that take solvent effects into account, for the purpose of supporting this assumption, are difficult to interpret correctly and have therefore not been performed; however, these remain options for future work. The general structures of the complexes 3d,k are very similar: both complexes feature a plane composed of four and three copper ions, respectively. Furthermore, each edge of this plane is bridged either only by triazole ligands or by both triazole ligands and iodide ions. The only true difference between these two complexes is the substitution pattern at the 4-position of the triazole ring, with complex 3k possessing a propyl residue, and with complex 3d featuring a phenyl ring instead. In the case of complex 3k, the larger steric bulk of the

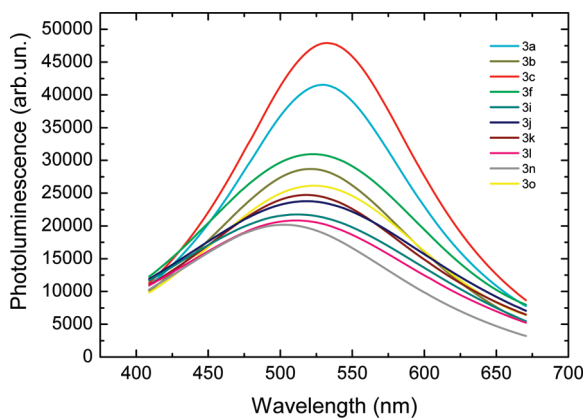


Figure 5. Experimental photoluminescence (arbitrary units) as function of wavelength (nm).

propyl substituent compared to the phenyl group is most likely the reason why this complex with three bridging triazole ligands was formed.

DFT CALCULATIONS

Density functional theory (DFT) studies on complexes **3a,k** were performed with the BP86 functional,²⁸ the def2-SV(P) basis set of Weigend and Ahlrichs,²⁹ and the Turbomole program package.³⁰ The resolution-of-identity (RI) approximation for the Coulomb energy and operator was employed in all ground-state energy calculations, using a self-consistent-field convergence threshold of 10^{-9} hartree and geometry convergence thresholds of 10^{-8} hartree and 10^{-5} hartree/bohr for the total energy and the Cartesian gradient, respectively. The numerical quadrature was performed on Turbomole's grid m4. Geometries with C_1 point-group symmetry for **3a** and C_3 point-group symmetry for **3k** were obtained. Note that the complex **3a** was computed as a neutral molecule, whereas **3k** was computed as a monocation. Analytic harmonic vibrational frequencies were computed to ensure that the optimized geometries are true minima, that is, do not show imaginary frequencies. Selected geometrical parameters of **3a,k** are compared with experimental values in Tables 3 and 5, respectively.

The theoretical and experimental geometries for **3a** are in fair agreement (Table 3). The theoretical equilibrium geometry appears to be slightly more symmetric than the experimental structure, as shown by the smaller difference between the calculated I(1)–Cu(1) and I(1)–Cu(1A) bond lengths. Also, the calculated P(1)–Cu(1)–I(1) and P(1)–Cu(1)–I(1A) bond angles are almost equal in magnitude, whereas the experimental X-ray structure shows a difference of almost 7° between these two angles.

The experimental X-ray structure of **3k** is much less symmetric than the gas-phase cation investigated in the DFT calculations, as demonstrated by the existence of three distinct experimental I(1)–Cu bond lengths and only one bond length in the DFT calculations (Table 5).

It is tempting to speculate about cuprophilicity in view of the relatively short computed copper–copper distances of about 2.6 Å, but note that all equilibrium structures have been optimized at the common gradient-corrected DFT level (BP86 functional). At this level, dispersion-type R^{-6} terms are not accounted for, and the BP86 functional unavoidably predicts repulsive behavior

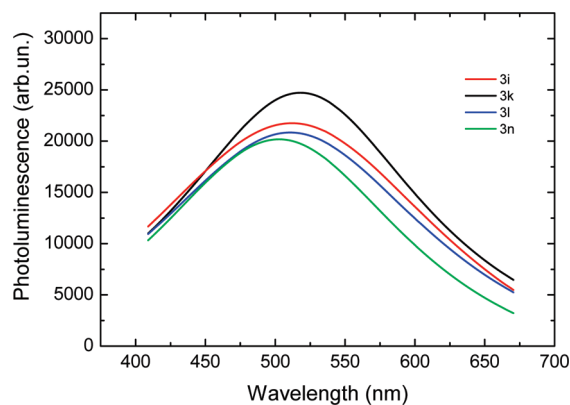


Figure 6. Photoluminescence spectra of complexes **3i,k,l,n**.

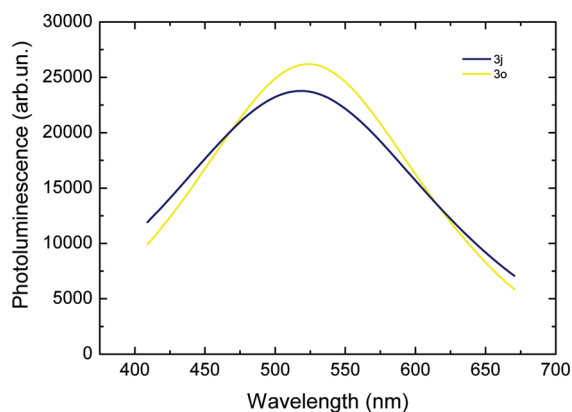


Figure 7. Photoluminescence spectra of the complexes **3j,o**.

between unsupported metalphilic fragments. Conversely, if a common gradient-corrected DFT method is able to reproduce an experimental structure, it should be clear that the interaction is not of the metalphilic type.³¹

SPECTRAL INVESTIGATION

For further characterization of the metal complexes, photoluminescence spectra of some of the complexes were examined. For this purpose, the individual complexes were dissolved in dichloromethane in equal molarity and spin-coated on a glass plate in order to guarantee a uniform layer thickness.

The photoluminescence of the selected complexes in Table 2 was measured as a function of the wavelength (Figure 5).

Complexes **3a,c**, with 4-(diphenylphosphino)-1,5-diphenyl-1*H*-1,2,3-triazole (**2a**) as the ligand and copper(I) chloride or iodide as the metal salt, exhibit the largest intensities, as shown in Figure 5. The luminescence of the other complexes is of lower intensity, with their maxima slightly shifted to lower wavelength in the range of 500–530 nm. Complexes **3a,c**, with 4-(diphenylphosphino)-1,5-diphenyl-1*H*-1,2,3-triazole (**2a**) as ligand, show luminescence peaks at approximately 530–540 nm, within the green range of the spectrum, and differ only slightly in the intensities and in the position of their maxima (Figure 5). The copper(I) chloride complex **3c** exhibits a somewhat higher intensity than the copper(I) iodide complex **3a**, which suggests that the halogen atom has little influence on the type and the intensity of the luminescence. When the phenyl substituent at the

C-5 atom of the triazole is replaced by a propyl substituent, the emission peak is shifted to 525 nm. Exchanging the phenyl substituent at the nitrogen atom in the 1-position of the triazole ring with a hexyl substituent or a 4-nitrophenyl substituent or, alternatively, replacing both phenyl substituents in the 1- and 5-positions by propyl and hexyl substituents, respectively, shifts the maximum into the short-wave range of the spectrum at around 500 nm (Figure 6). These results indicate that these substituents, by changing the electron density of the triazole unit as a result of their electron-pushing or mesomeric characteristics, account for an emission peak shifting to a higher energy region of the spectrum.

Similar conclusions can be derived from the photoluminescence curves of complex **3j**, with 4-(diphenylphosphino)-1-phenethyl-5-phenyl-1*H*-1,2,3-triazole (**2d**) as the ligand, and complex **3o**, with 5-(3-chlorophenyl)-4-(diphenylphosphino)-1-phenyl-1*H*-1,2,3-triazole (**2j**) as the ligand. Both substituents shift the maxima of the photoluminescence spectra into the short-wave range to 520–525 nm (Figure 7).

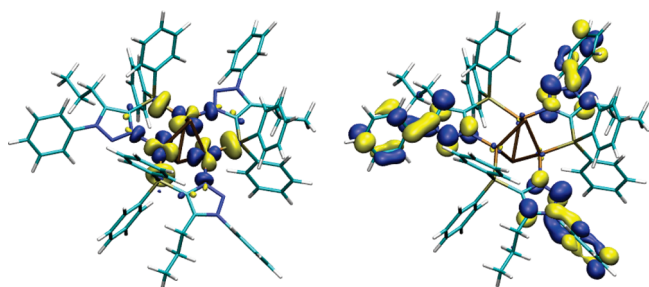


Figure 8. Calculated HOMO (left) and LUMO (right) of complex **3k**.

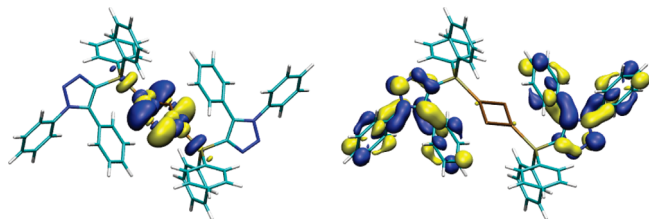


Figure 9. Calculated HOMO (left) and LUMO (right) of complex **3a**.

These results strongly suggest that, by using electron-rich substituents at all three positions of the triazole moiety, the intensity can be increased and the maximum of the luminescence can be shifted into the long-wave region of the spectrum. With the help of the electron-rich triazole or the electron-donating phosphine, the ligand can transfer a larger electron density to the metal core. These changes can be understood on the basis of HOMO–LUMO considerations. Similar to the case for other copper complexes, the highest occupied molecular orbital (HOMO) of the complex is mainly composed of metal orbitals, and the lowest unoccupied molecular orbital (LUMO) is located on the ligand sphere.³² An electron-rich triazole increases the energy of the HOMO by transfer of electron density, consequently making the HOMO–LUMO energy gap smaller and shifting the emission peak into the long-wave range of the spectrum. Likewise, lowering the HOMO energy by the use of electron-poor triazole ligands increases the HOMO–LUMO energy gap and leads to a shift of the maximum into the short-wave range of the spectrum. These assumptions were confirmed by density functional computations. At the BP86/def2-SV(P) level, the HOMO energies of **3a,k** are -4.1 and -6.0 eV, respectively. Emission is shifted by about 10–15 nm toward shorter wavelengths from **3a** to **3k**. It is evident from Figure 8 that the LUMO of the charged trinuclear complex resides on the ligand sphere. The HOMO consists mainly of one d orbital of each metal, as well as the lone pair electrons of the phosphorus atom and the bonding orbital

Table 7. HOMO–LUMO Energy Gaps (in eV) Computed at the BP86/def2-SV(P) and B3LYP/def2-SV(P) Levels for the Complexes **3a,k** at Their Ground-State Geometries and at the B3LYP Optimized Geometries of the Excited States

functional	ground state	lowest singlet excited state	lowest triplet excited state
Complex 3a			
BP86	1.79		
B3LYP	3.57	2.97	2.96
Complex 3k			
BP86	1.98		
B3LYP	3.82	3.39	3.39

Table 6. Vertical Absorptions and Emissions Computed at the B3LYP/def2-SV(P) TDDFT Level for the Complexes **3a,k**^a

state	absorption		emission	
	wavelength (nm)	character	wavelength (nm)	character
Complex 3a				
¹ A _g	406.2	97% HOMO → LUMO+1	510.2	99% HOMO → LUMO
¹ A _u	406.8	97% HOMO → LUMO	508.4	99% HOMO → LUMO+1
³ A _g	408.5	95% HOMO → LUMO+1	515.5	98% HOMO → LUMO
³ A _u	409.0	95% HOMO → LUMO	513.0	98% HOMO → LUMO+1
Complex 3k				
¹ A	375.1	69% HOMO → LUMO+1	433.4	92% HOMO → LUMO+1
¹ E	377.6	83% HOMO → LUMO	436.3	80% HOMO → LUMO
³ A	378.2	86% HOMO → LUMO+1	439.2	100% HOMO → LUMO+1
³ E	380.5	81% HOMO → LUMO	440.6	72% HOMO → LUMO, 21% HOMO → LUMO+1

^aThe point-group symmetries were restricted to C_i and C₃, respectively.

of the carbon–nitrogen π bond. The LUMO is mainly composed of antibonding orbitals of the triazole core and one phenyl substituent.

The HOMO and LUMO were also calculated for complex **3a**. Again, the HOMO was found to be on the metal center and the LUMO on the triazole ligand (Figure 9). In contrast to the case for the trinuclear complex **3k**, the HOMO consists mainly of the *d* orbitals of the metals and the nonbonding orbitals of the bridging halides with an admixture of the lone pair electrons of the phosphorus atoms of the two ligands. Similar to the case for the previous complex **3k**, the LUMO basically consists of antibonding orbitals of the triazole moiety.

Because the HOMO and LUMO reside on the metal clusters and ligand spheres, respectively, the electronic excitations discussed here are expected to be of metal-to-ligand charge transfer character (MLCT). DFT calculations of such excitations are known to be very difficult, if not impossible, especially with a functional that lacks exact exchange such as the BP86 functional. We have nevertheless attempted to compute absorption and emission spectra for complexes **3a,k** at the time-dependent DFT level (TDDFT) using the B3LYP functional,³³ which includes certain amounts of Hartree–Fock exchange, to obtain some qualitative insight into these excitations. The TDDFT calculations were performed with the Turbomole program package,³⁴ and the results are shown in Table 6.

In **3a**, the first two LUMOs in the ground-state geometry have a_g (LUMO) and a_u (LUMO+1) symmetry and are energetically nearly degenerate. Hence, the excitation energies come in pairs. In accord with the pronounced MLCT character, the singlet and triplet excitations are also very similar in energy. Despite the charge-transfer character, the longest computed emission wavelength (515.5 nm) is in reasonable agreement with experiment (ca. 530 nm). In **3k**, the three ligand LUMOs transform according to the irreducible representations *a* and *e* of the C_3 point group and are almost degenerate. The corresponding excitation energies are very similar and, as for **3a**, the pronounced MLCT character is reflected in the similar singlet and triplet excitation energies. **3k** displays much shorter wavelengths than **3a**, in accord with experiment and with its lower lying HOMO energy and larger HOMO–LUMO energy gap (Table 7). Although the quantitative agreement between the computed and measured emission wavelengths for **3k** is rather poor (which is not unexpected), the observed trends are captured correctly by the TDDFT calculations, which hint at pronounced MLCT-type excited states involving HOMO→LUMO(+1) orbital transitions.

CONCLUSION

In summary, phosphinotriazolyl ligands comprising a variety of aryl and alkyl substituents have been synthesized. Treatment of these potentially bidentate ligands with copper halides yielded a series of new emissive metal complexes possessing three different structural classes, mainly a charged trinuclear complex (**3k**) and, probably due to solvent effects or steric reasons, a dinuclear (**3a**) and a tetranuclear (**3d**) complex, respectively. Both the absorption and the corresponding emission peak positions of the di- and trinuclear complexes were measured, for which a rational explanation is provided by the HOMO/LUMO correlation via the assistance of computational approaches. We anticipate that such a design strategy might provide new insight into the preparation of group 11 fluorescent dyes

with good quantum yields and tunable emission hues that particularly fit into the current interest in OLEDs and related subjects.

CRYSTAL STRUCTURE STUDIES

Single-crystal X-ray diffraction studies were carried out on a Nonius Kappa-CCD diffractometer at 123(2) K using Mo $K\alpha$ radiation ($\lambda = 0.71073$ Å). Direct methods (**3k,d**) or Patterson methods (**3a**) (SHELXS-97)³⁵ were used for structure solution, non hydrogen atoms were refined anisotropically (full-matrix least-squares refinement on F^2 (SHELXL-97)). H atoms were refined using a riding model. Semiempirical absorption corrections were applied. In **3k** one propyl group and one CH_2Cl_2 solvent molecule were disordered.

Complex 3a: colorless crystals, $C_{52}H_{40}Cu_2I_2N_6P_2$, $M = 1191.72$, crystal size $0.45 \times 0.25 \times 0.15$ mm, triclinic, space group $P\bar{1}$ (No. 2), $a = 8.903(1)$ Å, $b = 9.894(2)$ Å, $c = 15.726(3)$ Å, $\alpha = 74.45(2)^\circ$, $\beta = 89.19(2)^\circ$, $\gamma = 65.38(2)^\circ$, $V = 1205.7(4)$ Å³, $Z = 1$, $\rho(\text{calcd}) = 1.641$ Mg m⁻³, $F(000) = 588$, $\mu = 2.271$ mm⁻¹, 26 882 reflections ($2\theta_{\text{max}} = 55^\circ$), 5477 unique reflections ($R_{\text{int}} = 0.049$), 289 parameters, $R1$ ($I > 2\sigma(I)$) = 0.032, $wR2$ (all data) = 0.088, GOF = 1.05, largest difference peak and hole 1.440 and -1.236 e Å⁻³.

Complex 3d: yellow crystals, $C_{52}H_{40}Cu_4I_4N_6P_2 \cdot C_4H_{10}O$, $M = 1646.72$, crystal size $0.25 \times 0.15 \times 0.10$ mm, monoclinic, space group $P2_1/c$ (No. 15), $a = 24.312(3)$ Å, $b = 9.928(1)$ Å, $c = 25.220(3)$ Å, $\beta = 108.98(1)^\circ$, $V = 5756.4(11)$ Å³, $Z = 4$, $\rho(\text{calcd}) = 1.900$ Mg m⁻³, $F(000) = 3176$, $\mu = 3.703$ mm⁻¹, 35 230 reflections ($2\theta_{\text{max}} = 55^\circ$), 6576 unique reflections ($R_{\text{int}} = 0.089$), 330 parameters, $R1$ ($I > 2\sigma(I)$) = 0.057, $wR2$ (all data) = 0.151, GOF = 1.08, largest difference peak and hole 1.969 and -2.873 e Å⁻³.

Complex 3k: yellow crystals, $[C_{69}H_{66}Cu_3I_2N_9P_3]^+ \cdot 0.5[Cu_2I_4]^- \cdot 2CH_2Cl_2$, $M = 2045.83$, crystal size $0.24 \times 0.18 \times 0.06$ mm, monoclinic, space group $P2_1/c$ (No. 14), $a = 14.341(1)$ Å, $b = 16.446(2)$ Å, $c = 32.859(4)$ Å, $\beta = 93.29(1)^\circ$, $V = 7737.1(14)$ Å³, $Z = 4$, $\rho(\text{calcd}) = 1.756$ Mg m⁻³, $F(000) = 4000$, $\mu = 2.927$ mm⁻¹, 52 479 reflections ($2\theta_{\text{max}} = 55^\circ$), 17 114 unique reflections ($R_{\text{int}} = 0.054$), 871 parameters, 1248 restraints, $R1$ ($I > 2\sigma(I)$) = 0.094, $wR2$ (all data) = 0.207, GOF = 1.28, largest difference peak and hole 2.528 and -1.914 e Å⁻³. Due to the bad quality of the data and the disorder, in addition to geometrical restraints and constraints for the displacement parameters for the disordered parts, general restraints for the displacement parameters were applied. However, the structure was unequivocally determined.

Crystallographic data (excluding structure factors) for the structures reported in this work have been deposited with the Cambridge Crystallographic Data Centre as Supplementary Publication Nos. CCDC 801004 (**3a**), CCDC 801005 (**3k**), and CCDC 801006 (**3d**). Copies of the data can be obtained free of charge on application to The Director, CCDC, 12 Union Road, Cambridge CB2 1EZ, U.K. (fax, int. code+(1223)336-033; e-mail, deposit@ccdc.cam.ac.uk).

ASSOCIATED CONTENT

S Supporting Information. CIF files giving crystallographic data for compounds **3a** (CCDC-801004), **3k** (CCDC-801005), and **3d** (CCDC-801006) (CIF-format), text and figures giving details of the syntheses and characterization data for the compounds prepared in this paper, and tables giving Cartesian coordinates (in Å) of the optimized BP86/def2-SV(P) and B3LYP/def2-SV(P) ground-state equilibrium geometries of the compounds **3a,k**. This material is available free of charge via the Internet at <http://pubs.acs.org>.

AUTHOR INFORMATION

Corresponding Author

*E-mail: braese@kit.edu (S.B.); baumann@cynora.de (T.B.).

ACKNOWLEDGMENT

Financial support from the KIT is acknowledged. W.K. and S.B. thank the Deutsche Forschungsgemeinschaft (DFG) for support through projects C1 and B2 of SFB/TRR 88 (“Kooperative Effekte in homo- und heterometallischen Komplexen”).

REFERENCES

- (1) (a) Evans, R. C.; Douglas, P.; Winscom, C. J. *Coord. Chem. Rev.* **2006**, *250*, 2093. (b) Yang, C.-H.; Cheng, Y.-M.; Chi, Y.; Hsu, C.-J.; Fang, F.-C.; Wong, K.-T.; Chou, P.-T.; Chang, C.-H.; Tsai, M.-H.; Wu, C.-C. *Angew. Chem., Int. Ed.* **2007**, *46*, 2418. (c) Chang, C.-F.; Cheng, Y.-M.; Chi, Y.; Chiu, Y.-C.; Lin, C.-C.; Lee, G.-H.; Chou, P.-T.; Chen, C.-C.; Chang, C.-H.; Wu, C.-C. *Angew. Chem., Int. Ed.* **2008**, *47*, 4542. (d) Williams, J. A. G.; Develay, S.; Rochester, D. L.; Murphy, L. *Coord. Chem. Rev.* **2008**, *252*, 2596. (e) Che, C.-M.; Kwok, C.-C.; Lai, S.-W.; Rausch, A.-F.; Finkenzeller, W.-J.; Zhu, N.; Yersin, H. *Chem. Eur. J.* **2010**, *16*, 233.
- (2) (a) O'Regan, B.; Grätzel, M. *Nature* **1991**, *353*, 737. (b) Mozer, A. J.; Griffith, M. J.; Tsekouras, G.; Wagner, P.; Wallace, G. G.; Mori, S.; Sunahara, K.; Miyashita, M.; Earles, J. C.; Gordon, K. C.; Du, L.; Katoh, R.; Furube, A.; Officer, D. L. *J. Am. Chem. Soc.* **2009**, *131*, 15621.
- (3) McMillin, D. R.; McNett, K. M. *Chem. Rev.* **1998**, *98*, 1201.
- (4) Shi, L.; Li, B.; Lu, S.; Zhu, D.; Li, W. *Appl. Organomet. Chem.* **2009**, *23*, 379.
- (5) Lin, Y.-Y.; Chan, S.-C.; Chan, W. M. C.; Hou, Y.-J.; Zhu, N.; Che, C.-M.; Liu, Y.; Wang, Y. *Chem. Eur. J.* **2003**, *9*, 1263.
- (6) Chou, P.-T.; Chi, Y. *Chem. Eur. J.* **2007**, *13*, 380.
- (7) Baranoff, E.; Yum, J. H.; Grätzel, M.; Nazeeruddin, Md. K. *J. Organomet. Chem.* **2009**, *694*, 2661.
- (8) Barbieri, A.; Accorsi, G.; Armaroli, N. *Chem. Commun.* **2008**, *19*, 2185.
- (9) (a) Zhang, Q.; Zhou, Q.; Cheng, Y.; Wang, L.; Ma, D.; Jing, X.; Wang, F. *Adv. Mater.* **2004**, *16*, 432. (b) Armaroli, N.; Accorsi, G.; Holler, M.; Moudam, O.; Nierengarten, J.-F.; Zhou, Z.; Wegh, R. T.; Welter, R. *Adv. Mater.* **2006**, *18*, 1313. (c) Xia, H.; He, L.; Zhang, M.; Zeng, M.; Wang, X.; Lu, D.; Ma, Y. *Opt. Mater.* **2007**, *29*, 667. (d) Qin, L.; Zhang, Q.; Sun, W.; Wang, J.; Lu, C.; Cheng, Y.; Wang, L. *Dalton Trans.* **2009**, *43*, 9388. (e) Tsuboyama, A.; Kuge, K.; Furugori, M.; Okada, S.; Hoshino, M.; Ueno, K. *Inorg. Chem.* **2007**, *46*, 1992. (f) Moudam, O.; Kaeser, A.; Delavaux-Nicot, B.; Duhayon, C.; Holler, M.; Accorsi, G.; Armaroli, N.; Ségué, I.; Navarro, J.; Destruel, P.; Nierengarten, J.-F. *Chem. Commun.* **2007**, 3077.
- (10) Felici, M.; Contreras-Carballada, P.; Vida, Y.; Smits, J. M. M.; Nolte, R. J. M.; De Cola, L.; Williams, R. M.; Feiters, M. C. *Chem. Eur. J.* **2009**, *15*, 13124.
- (11) Ahn, S. Y.; Ha, Y. *Mol. Cryst. Liq. Cryst.* **2009**, *204*, 59.
- (12) Chang, S.-Y.; Kavitha, J.; Li, S.-W.; Hsu, C.-S.; Chi, Y.; Yeh, Y.-S.; Chou, P.-T.; Lee, G.-H.; Carty, A. J.; Tao, Y.-T.; Chien, C.-H. *Inorg. Chem.* **2006**, *45*, 137.
- (13) Tung, Y.-L.; Wu, P.-C.; Liu, C.-S.; Chi, Y.; Yu, J.-K.; Hu, Y.-H.; Chou, P.-T.; Peng, S.-M.; Lee, G.-H.; Tao, Y.; Carty, A. J.; Shu, C.-F.; Wu, F.-I. *Organometallics* **2004**, *23*, 3745.
- (14) Manbeck, G. F.; Bennesel, W. W.; Evans, C. M.; Eisenberg, R. *Inorg. Chem.* **2010**, *49*, 2834.
- (15) Krasinski, A.; Fokin, V. V.; Sharpless, K. B. *Org. Lett.* **2004**, *6*, 1237.
- (16) Liu, D.; Gao, W.; Dai, Q.; Zhang, X. *Org. Lett.* **2005**, *7*, 4907.
- (17) Wang, K.-W.; Chen, J.-L.; Cheng, Y.-M.; Chung, M.-W.; Hsieh, C.-C.; Lee, G.-H.; Chou, P.-T.; Chen, K.; Chi, Y. *Inorg. Chem.* **2010**, *49*, 1372.
- (18) Mauro, M.; Procopio, E. Q.; Sun, Y.; Chien, C.-H.; Donghi, D.; Panigati, M.; Mercandelli, P.; Mussini, P.; D'Alfonso, G.; De Cola, L. *Adv. Funct. Mater.* **2009**, *19*, 2607.
- (19) Zink, D. M.; Baumann, T.; Nieger, M.; Bräse, S. *Eur. J. Inorg. Chem.* **2011**, *8*, 1432–1437.
- (20) Soloveichik, G. L.; Eisenstein, O.; Poulton, J. T.; Streib, W. E.; Huffman, J. C.; Caulton, K. G. *Inorg. Chem.* **1992**, *31*, 3306.
- (21) (a) Johnson, K.; Steed, J. W. *Dalton Trans.* **1998**, *16*, 2601. (b) Lastra, E.; Gamasa, M. P.; Gimeno, J.; Lanfranchi, M.; Tiripicchio, A. *Dalton Trans.* **1989**, *8*, 1499.
- (22) Larssonneur-Galibert, A. M.; Castan, P.; Jaud, J.; Bernardinelli, G. *Transition Met. Chem.* **1996**, *21*, 546.
- (23) Mézailles, N.; Le Floch, P.; Waschbüsch, K.; Ricard, L.; Mathey, F.; Kubiak, C. P. *J. Organomet. Chem.* **1997**, *541*, 277.
- (24) Fu, W.-F.; Gan, X.; Che, C.-M.; Cao, Q.-Y.; Zhou, Z.-Y.; Zhu, N. *N.-Y. Chem. Eur. J.* **2004**, *10*, 2228.
- (25) Camus, A.; Nardin, G.; Randaccio, L. *Inorg. Chim. Acta* **1975**, *12*, 23.
- (26) Zhou, W.-B.; Dong, Z.-C.; Song, J.-L.; Zeng, H.-Y.; Cao, R.; Guo, G.-C.; Huang, J.-S.; Li, J. J. *Cluster Sci.* **2002**, *13*, 119.
- (27) Nardin, G.; Randaccio, L.; Zangrando, E. *J. Chem. Soc., Dalton Trans.* **1975**, 2566.
- (28) (a) Becke, A. D. *Phys. Rev. A* **1988**, *38*, 3098. (b) Perdew, J. P. *Phys. Rev. B* **1986**, *33*, 8822. (c) Perdew, J. P. *Phys. Rev. B* **1986**, *34*, 7406.
- (29) Weigend, F.; Ahlrichs, R. *Phys. Chem. Chem. Phys.* **2005**, *7*, 3297.
- (30) Turbomole V6.0, a development of Universität Karlsruhe (TH) and Forschungszentrum Karlsruhe GmbH, 1989–2007, and TURBO-MOLE GmbH, since 2007. Available from <http://www.turbomole.com>, 2009.
- (31) Poblet, J.-M.; Bénard, M. *Chem. Commun.* **1998**, 1179.
- (32) Zhang, L.; Li, B.; Su, Z. *J. Phys. Chem. C* **2009**, *113*, 13968.
- (33) (a) Becke, A. D. *J. Chem. Phys.* **1993**, *98*, 5648. (b) Stephens, P. J.; Devlin, F. J.; Chabalowski, C. F.; Frisch, M. J. *J. Phys. Chem.* **1994**, *98*, 11623.
- (34) (a) Furche, F.; Rappoport, D. In *Computational Photochemistry*; Olivucci, M., Ed.; Elsevier: Amsterdam, 2005. (b) Furche, F.; Ahlrichs, R. *J. Chem. Phys.* **2002**, *117*, 7433. (c) Furche, F.; Ahlrichs, R. *J. Chem. Phys.* **2004**, *121*, 12772 (erratum).
- (35) Sheldrick, G. M. *Acta Crystallogr., Sect. A* **2008**, *64*, 112.